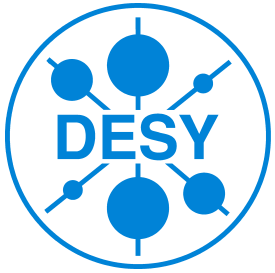

Proton Structure

S. Glazov

DESY

LP2009, Hamburg, 17 August 2009.

Proton structure probe

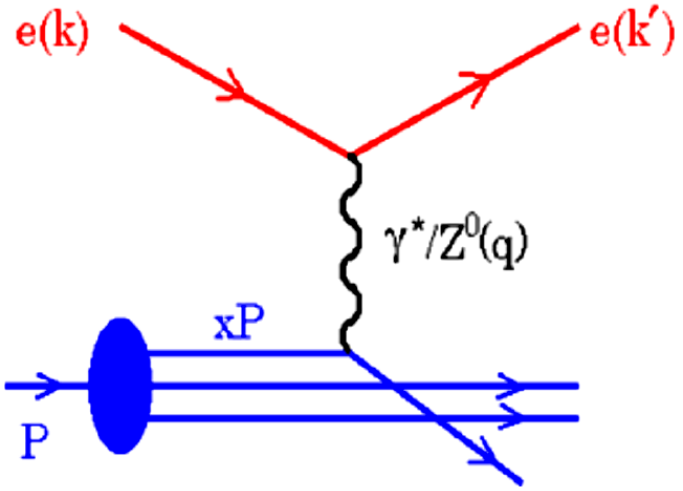

Neutral current Deep Inelastic Scattering (DIS) cross section:

$$\frac{\mathrm{d}^2\sigma^{\pm}}{\mathrm{d}x\mathrm{d}Q^2} = \frac{2\pi\alpha^2 Y_+}{Q^4 x}\sigma_r^{\pm} =$$

$$= \frac{2\pi\alpha^2 Y_+}{Q^4 x}\left[F_2(x,Q^2) - \frac{y^2}{Y_+}F_L(x,Q^2) \mp \frac{Y_-}{Y_+}xF_3\right]$$

where factors $Y_{\pm} = 1 \pm (1-y)^2$ and y^2 define polarisation of the exchanged boson and $y = Q^2/(S\,x)$.

Kinematics of inclusive scattering is determined by Q^2 and Bjorken x.
At leading order:

$$\begin{aligned} F_2 &= x\sum e_q^2(q(x)+\bar{q}(x)) \\ xF_3 &= x\sum 2e_q a_q(q(x)-\bar{q}(x)) \\ \sigma^+_{\mathrm{CC}} &\sim x(\bar{u}+\bar{c}) + x(1-y)^2(d+s) \\ \sigma^-_{\mathrm{CC}} &\sim x(u+c) + x(1-y)^2(\bar{d}+\bar{s}) \end{aligned}$$

$xg(x)$ — from F_2 scaling violation, jets and F_L

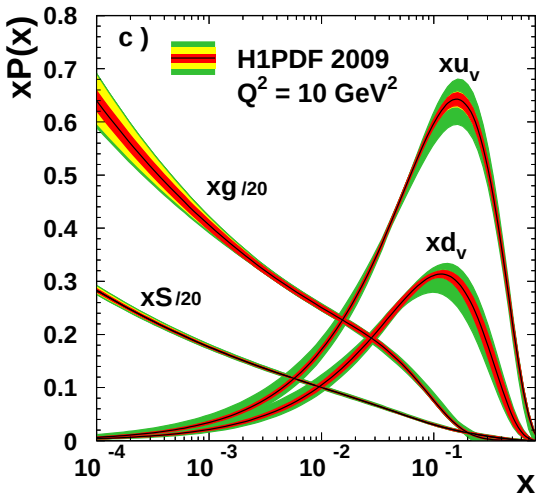

Moon, 1969.

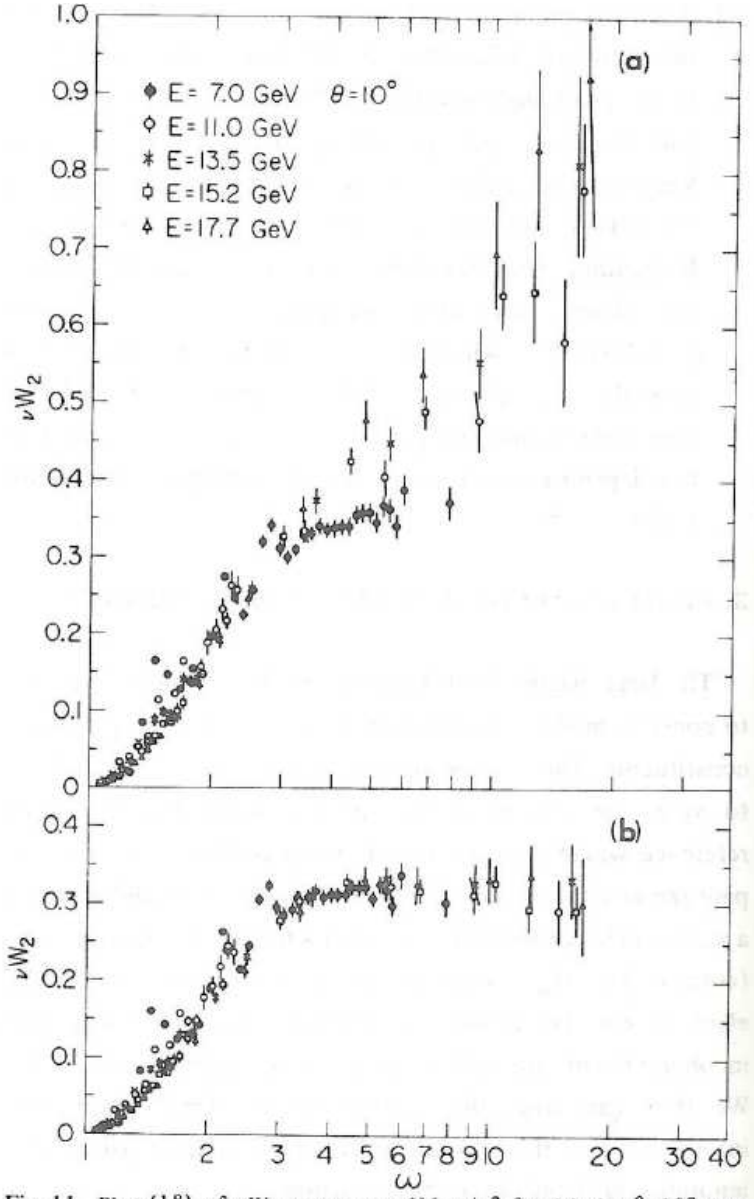

Fig. 11. Plots[18] of νW_2 versus $\omega = 2M_N\nu/q^2$ for (a) the $\theta=10°$ data for $R=\infty$; (b) the $\theta = 10°$ data for $R = 0$.

"The obvious way to test if νW_2 ($= F_2$) is only a function of $\omega = 2M_N\nu/q^2$ ($= 1/x$) is to plot each of the data points versus ω and see if one gets a single "universal curve" ... Since these plots were made before it was established that $R = \sigma_S/\sigma_T$ is small, the two extreme cases $R = \infty$ ($F_L = F_2$) and $R = 0$ ($F_L = 0$) were used to calculate νW_2. Clearly, for $R = 0$ one has a very striking "universal curve" for 10° data."

F. J. Gilman, EP69.

Clear evidence of non-elementarity of the proton.

One more step in the thousands year long quest of humanity to find the elementary building blocks of nature.

Experimental Data on the Proton Structure

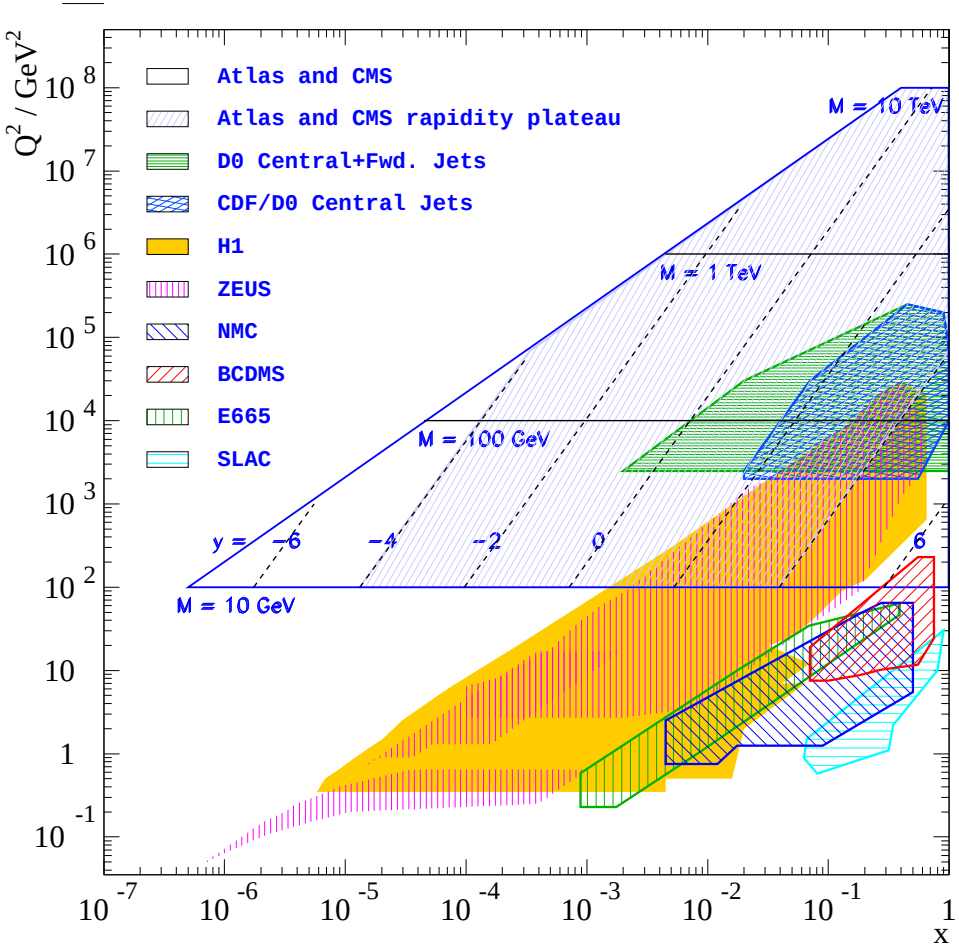

Persistent experimental effort over the last four decades, supported by theoretical developments (LO-NLO-NNLO-).
Huge extension of the knowledge due to the HERA collider.

- Large extension of the explored space in x, Q^2 vs the original SLAC results.
- PDFs + (N)LO DGLAP evolution equations are used for precise predictions for the LHC.

HERA, H1 and ZEUS. 1992-2007.

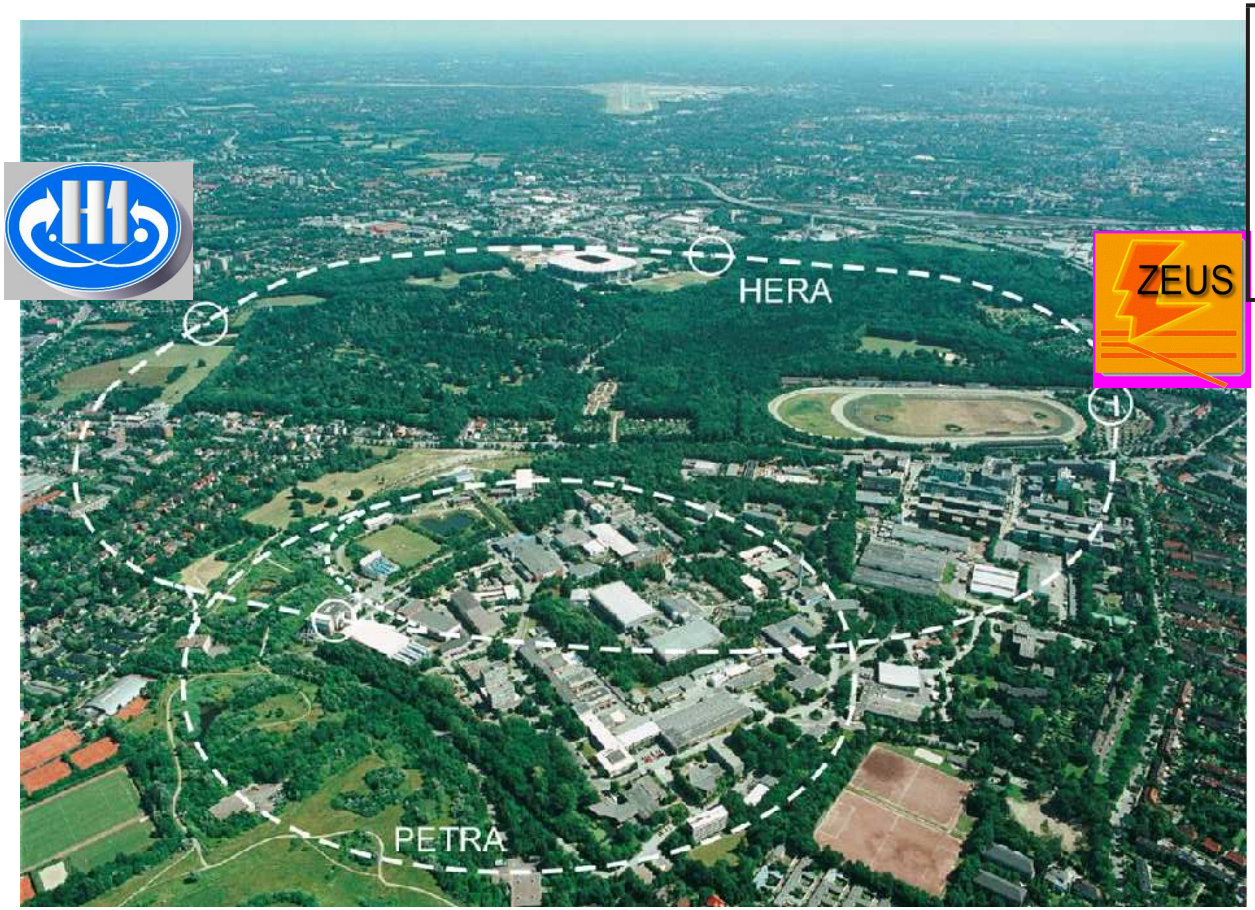

$E_e \times E_p = 27.5 \times 920\ \mathrm{GeV}^2$

$\sqrt{s} = 318\ \mathrm{GeV}$

$\mathrm{L} = 5 \cdot 10^{31} \mathrm{cm}^{-2} \mathrm{s}^{-1}$

e beam polarisation.

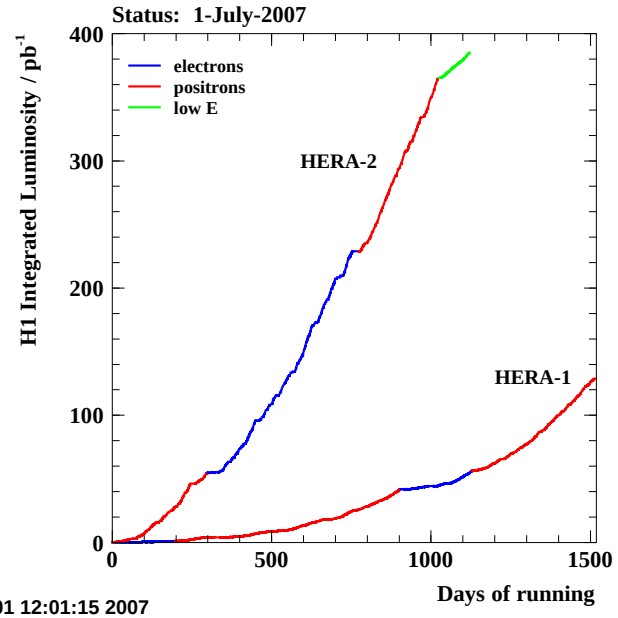

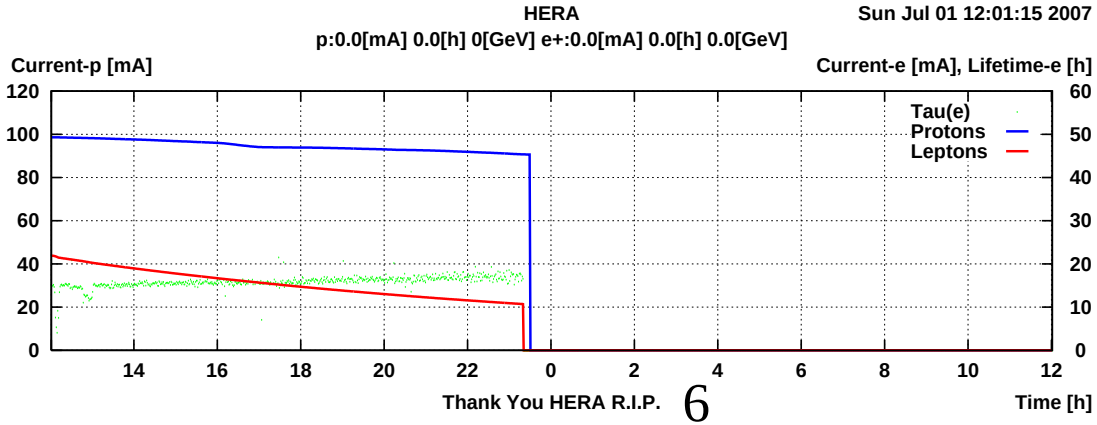

$ep \to eX$ Cross Section at low x and low Q^2

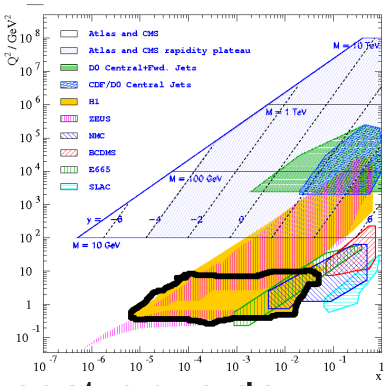

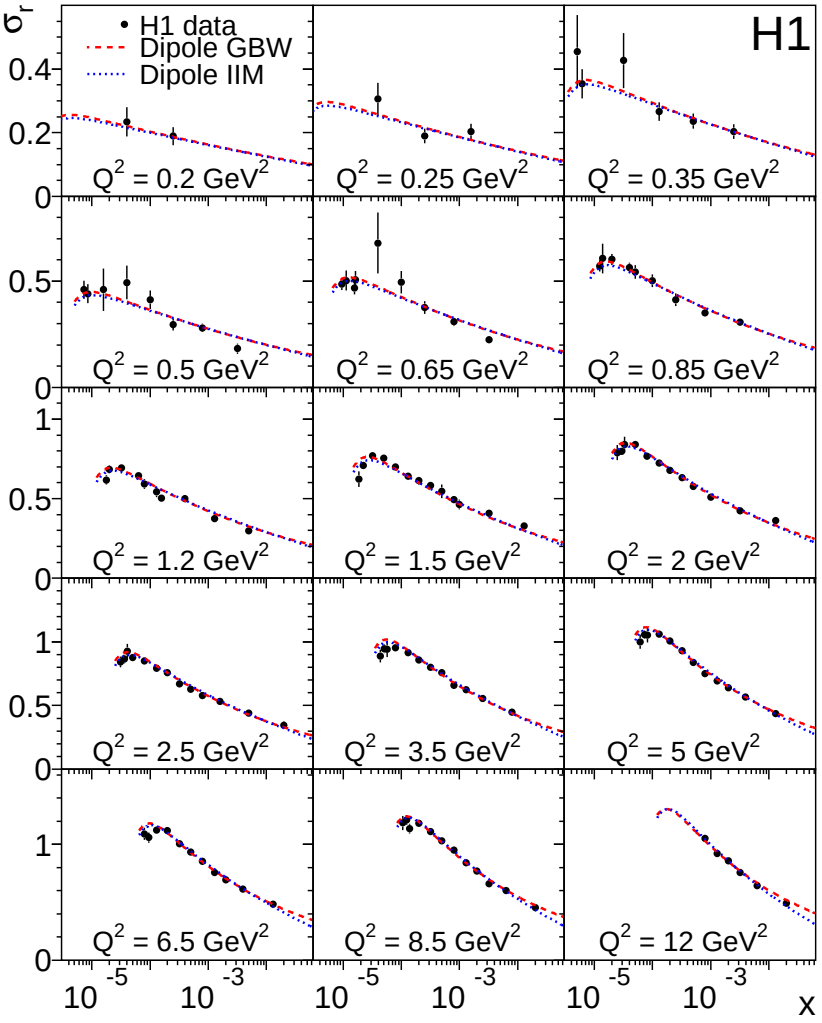

- At low Q^2 DIS cross section is defined by the structure functions F_2 and F_L

$$\sigma_r = F_2 - \frac{y^2}{1+(1-y)^2} F_L,$$

turn-over at lowest x is due to F_L.

- H1 data probes transition from photoproduction to DIS, complements ZEUS data (J. Breitweg *et al.*, Phys.Lett.B**487**, 53(2000)) which accesses even lower Q^2.
- Colour Dipole models describe the data well.

arXiv:0904.3513, submitted to EPJ

Structure Function F_2 at low x, medium Q^2

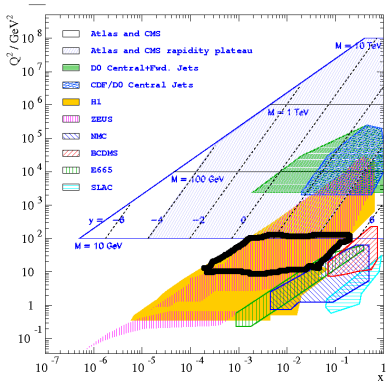

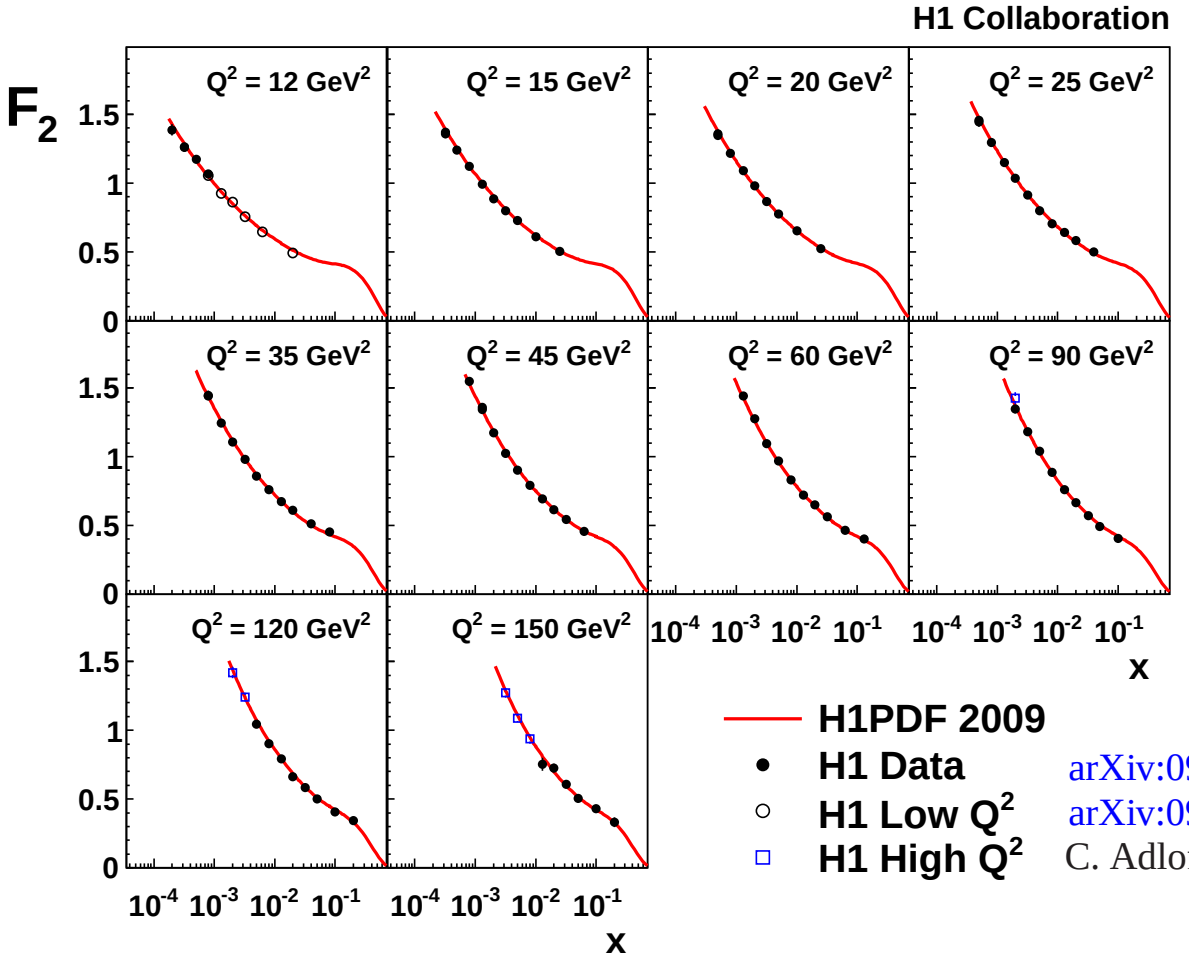

- Measurement of F_2 in perturbative region.
- HERA-I data, ~ 1.3% total precision.

arXiv:0904.3513, submitted to EPJ
arXiv:0904.0929, submitted to EPJ
C. Adloff *at al.* Eur.Phys.J. C30, 1 (2003)

$F_2(x, Q^2)$ shows strong rise as $x \to 0$, the rise increases with increasing Q^2.

F_2 Scaling violation at low x

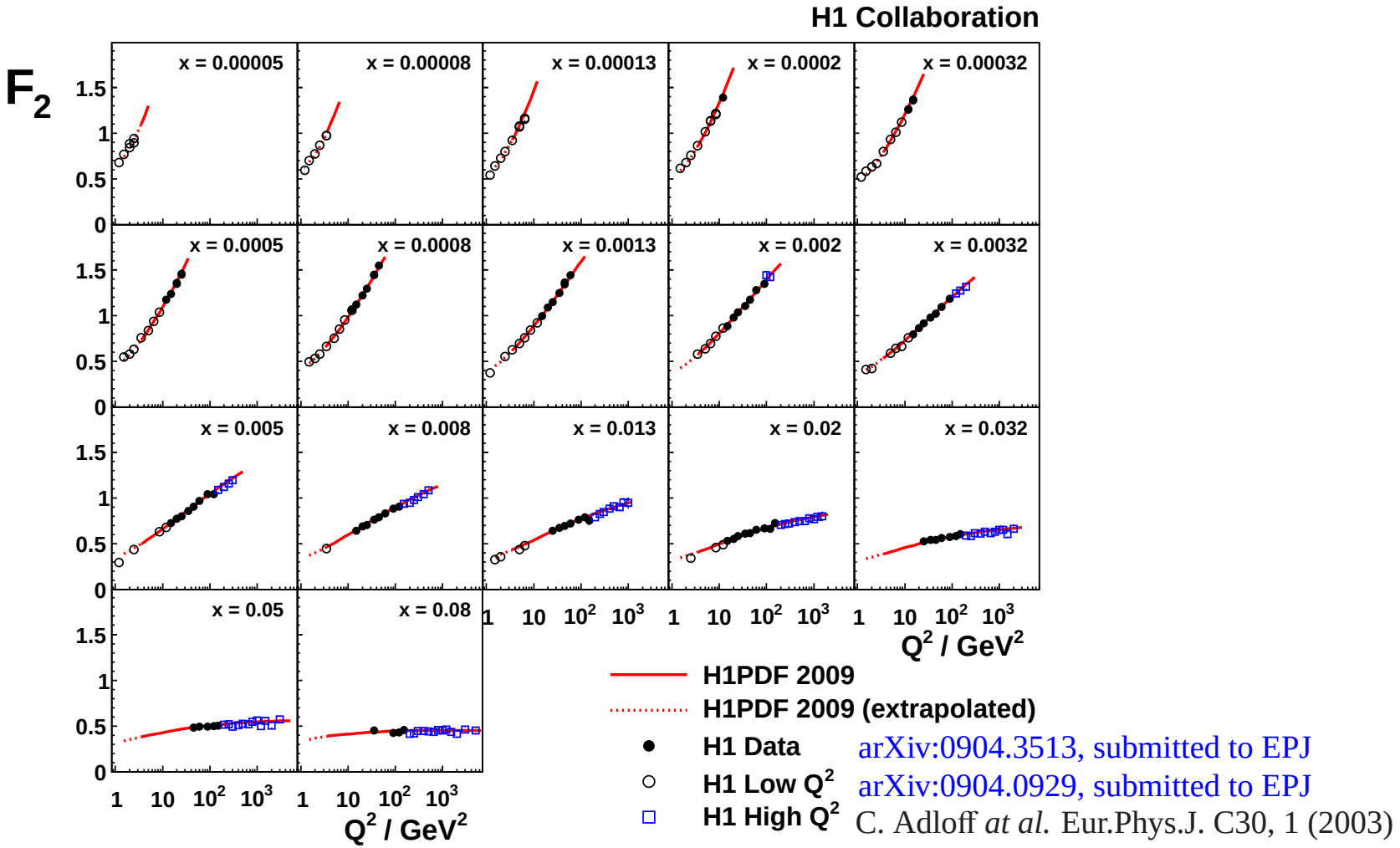

Large scaling violation at low x — large gluon density. Good agreement between the data and NLO QCD.

H1PDF2009 QCD Fit

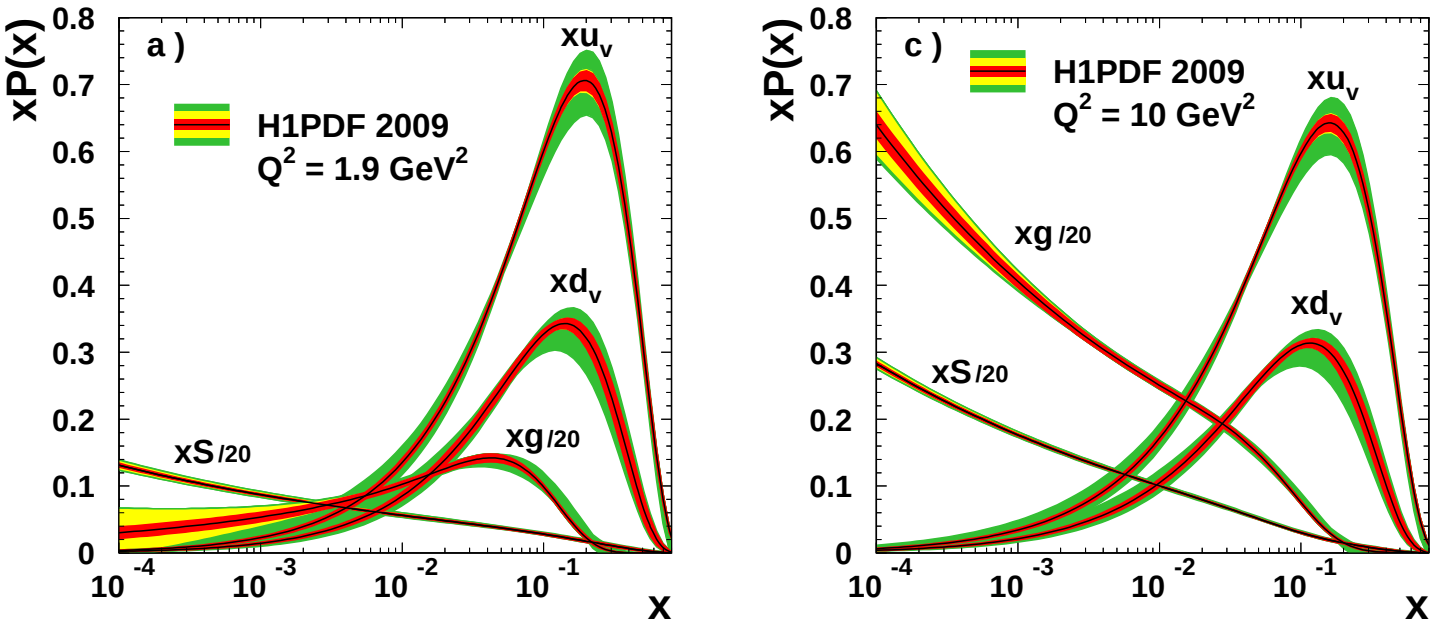

High experimental precision at low x.

Novel decomposition of sources of uncertainty.

- Parameterise PDFs at the starting scale $Q_0^2 = 1.9\ \mathrm{GeV}^2$ as $Ax^B(1-x)^c(1+Dx+...)$, evolve to higher scales following NLO DGLAP (using QCDNUM program) with TR treatment of heavy flavours, and compare with the H1 data.
- **Experimental** errors using $\delta\chi^2 = 1$ criterion.
- **Model** errors from variation of theory parameters like Q_0^2, m_C, m_b.
- **Parameterisation** errors from extra $D, E, ...$ terms in the parameterisation.

Sea and **g**luon dominate at low x. $xS > xg$ at the starting scale and $xg > xS$ at Q^2=10 GeV^2.

Measurement of the Structure Function F_L.

- In quark-parton model $F_L = 0$ for spin 1/2 quarks.
- In QCD $F_L > 0$ due to gluon emission. Large $xg(x)$ at low x implies sizable $F_L \rightarrow F_L$ is crucial test of QCD.
- Reduced proton beam energy runs at the end of HERA operation dedicated to measure F_L.

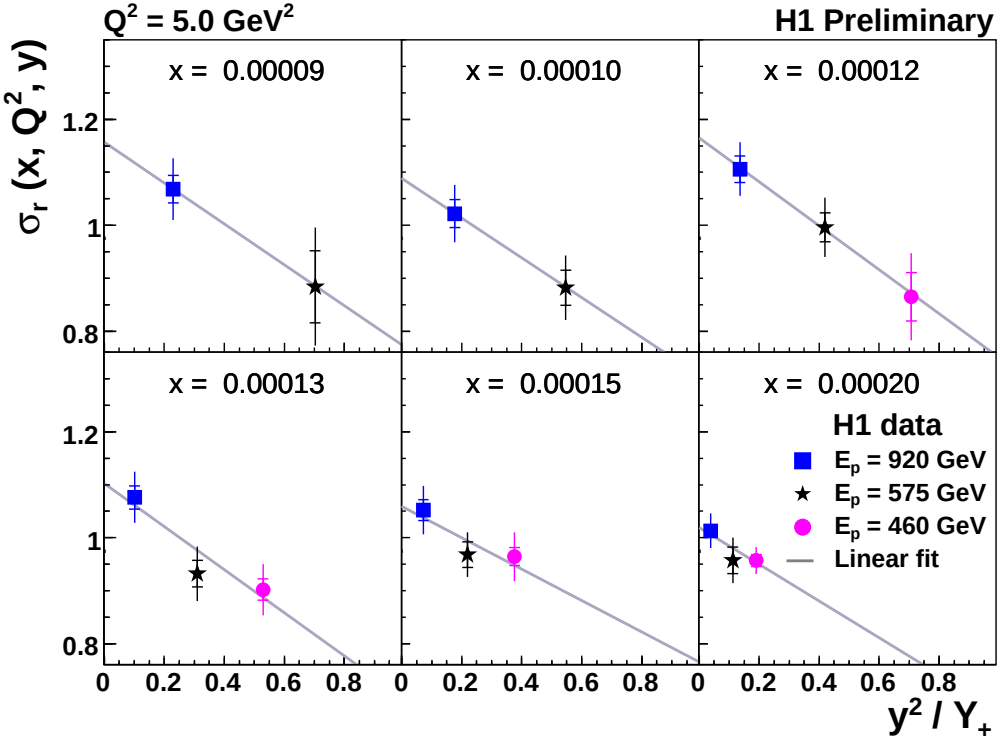

$$\sigma_r(y) = F_2 - \frac{y^2}{1+(1-y)^2} F_L$$

- Linear fit to the data at different centre-of-mass energies to obtain F_2 and F_L
- Relative normalisation from low y data

Published H1 and ZEUS F_L results

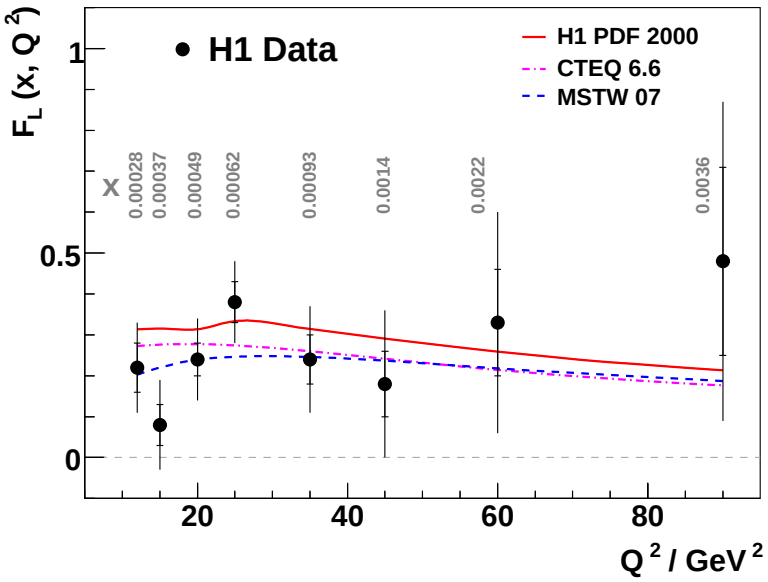

Phys.Lett. **B665** 139, 2008.

ZEUS

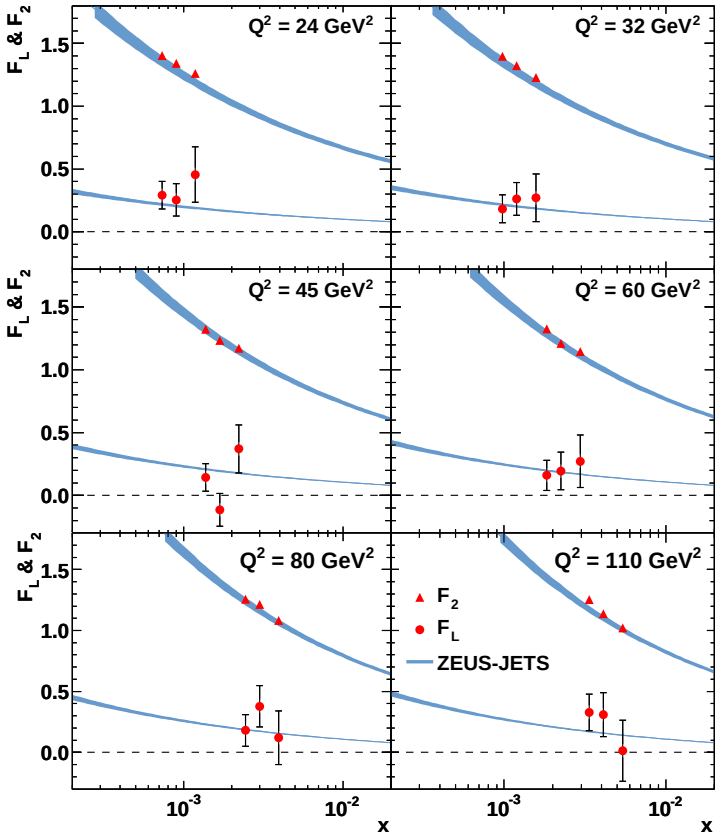

DESY-09-046, to be published in Phys. Lett. B

Both H1 and ZEUS collaborations published their first measurements of F_L. ZEUS also published F_2 extracted without any assumption on F_L.

F_L measured by H1

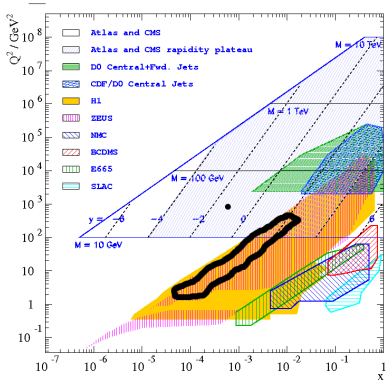

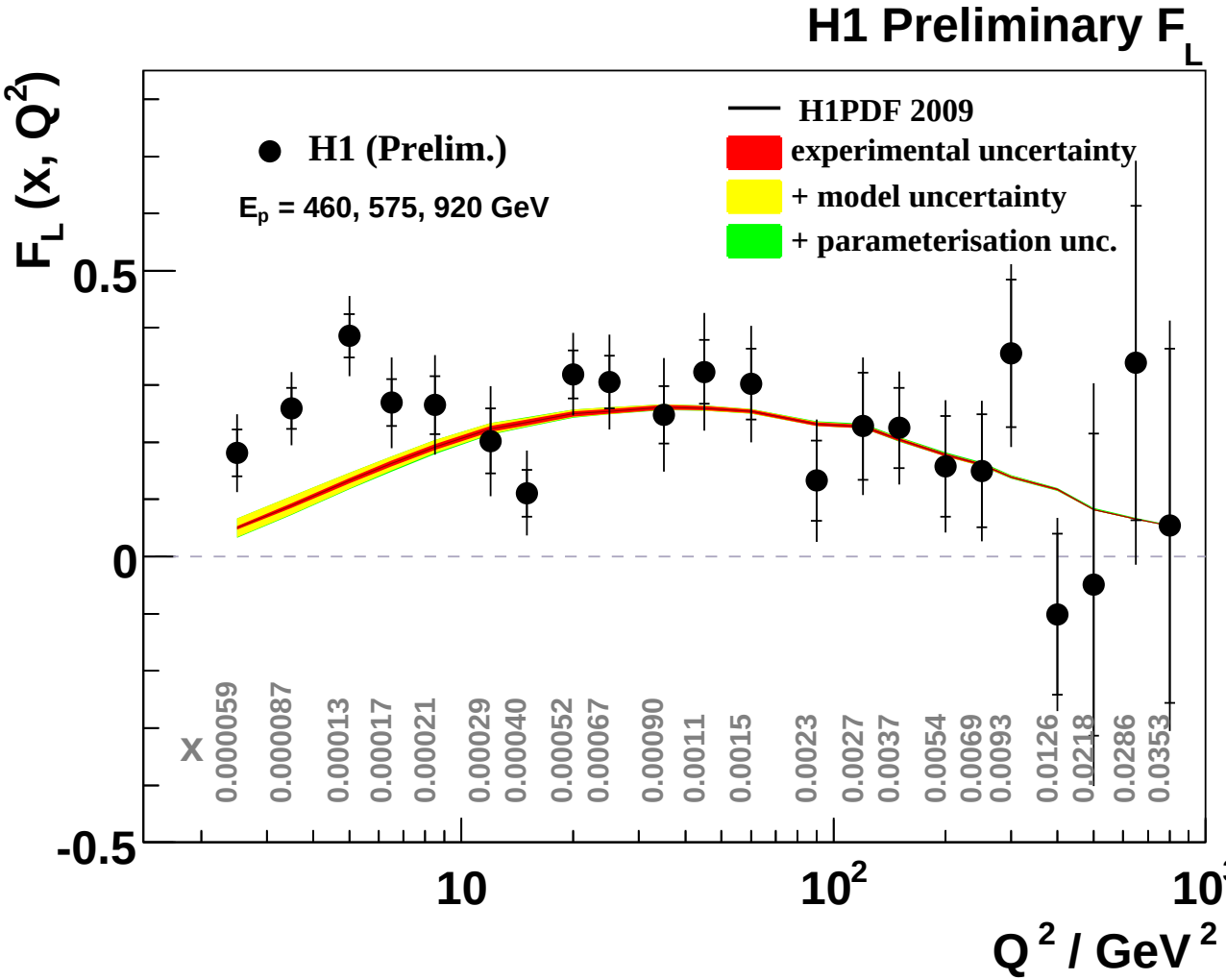

Extension to high $Q^2 \geq 90$ GeV^2 using LAr calorimeter and to low $Q^2 \leq 12$ GeV^2 using dedicated silicon tracker.

H1 measurements cover $2.5 \leq Q^2 \leq 800$ GeV^2 and $0.00005 \leq x \leq 0.04$ range
For $Q^2 \geq 10$ GeV^2, agree well with H1PDF 2009 prediction.

F_L measured at $Q^2 < 100$ GeV^2

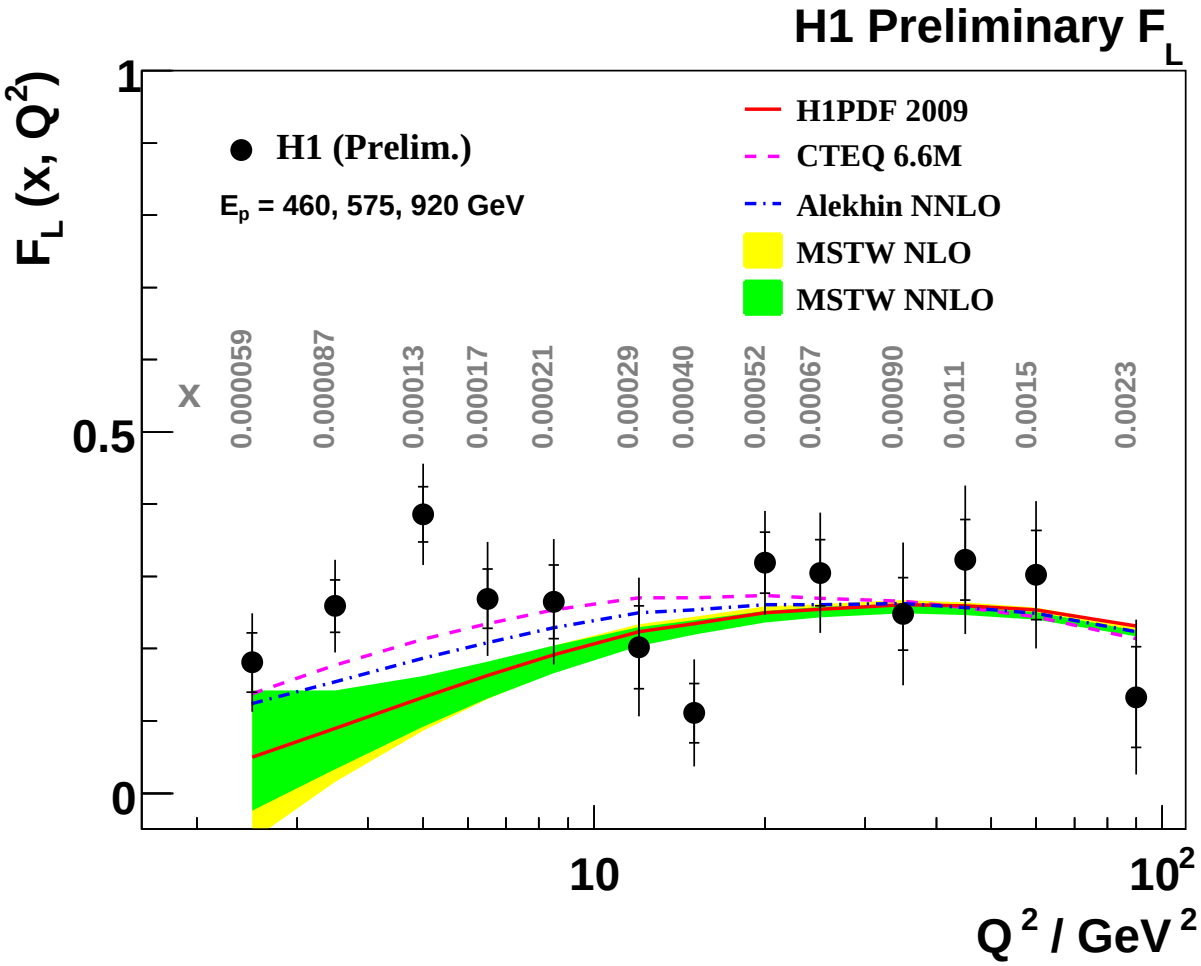

For $Q^2 < 10$ GeV^2 F_L acquires sizable higher order corrections.

MSTW and H1PDF 2009 predictions use the same scheme to calculate F_L. Data agree better with calculation of CTEQ and Alekhin.

DIS jet cross section

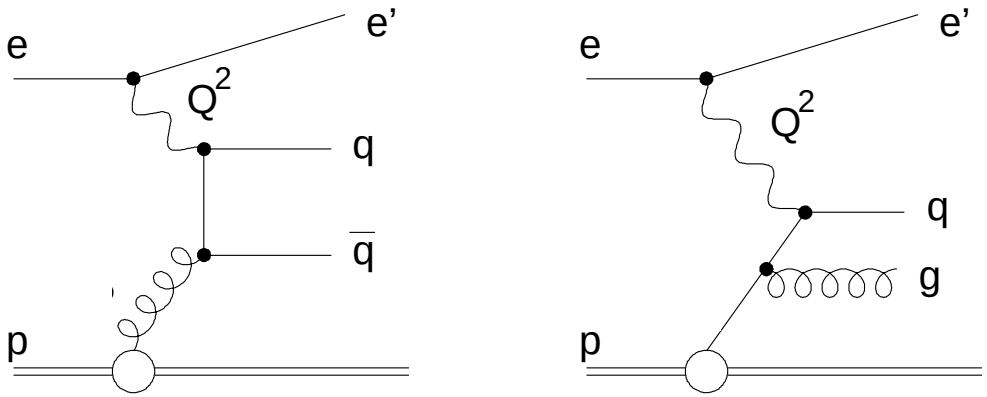

High P_t jets provide information on $xg(x)$ and α_S.

H1 Analysis based on complete HERA sample (395 pb^{-1}).

$\alpha_S(M_Z) = 0.1168 \pm 0.0007$ (exp)
$^{+0.0046}_{-0.0030}$ (th.) $\pm$ 0.0016 (PDF).

arXiv:0904.3870, Submitted to EPJC.

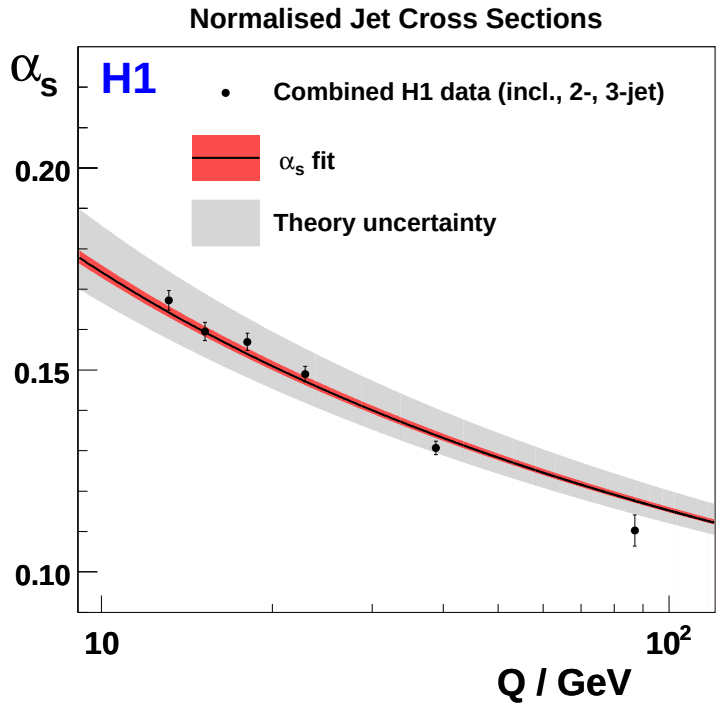

Uncertainty in higher order corrections dominate the errors

Combination of HERA data

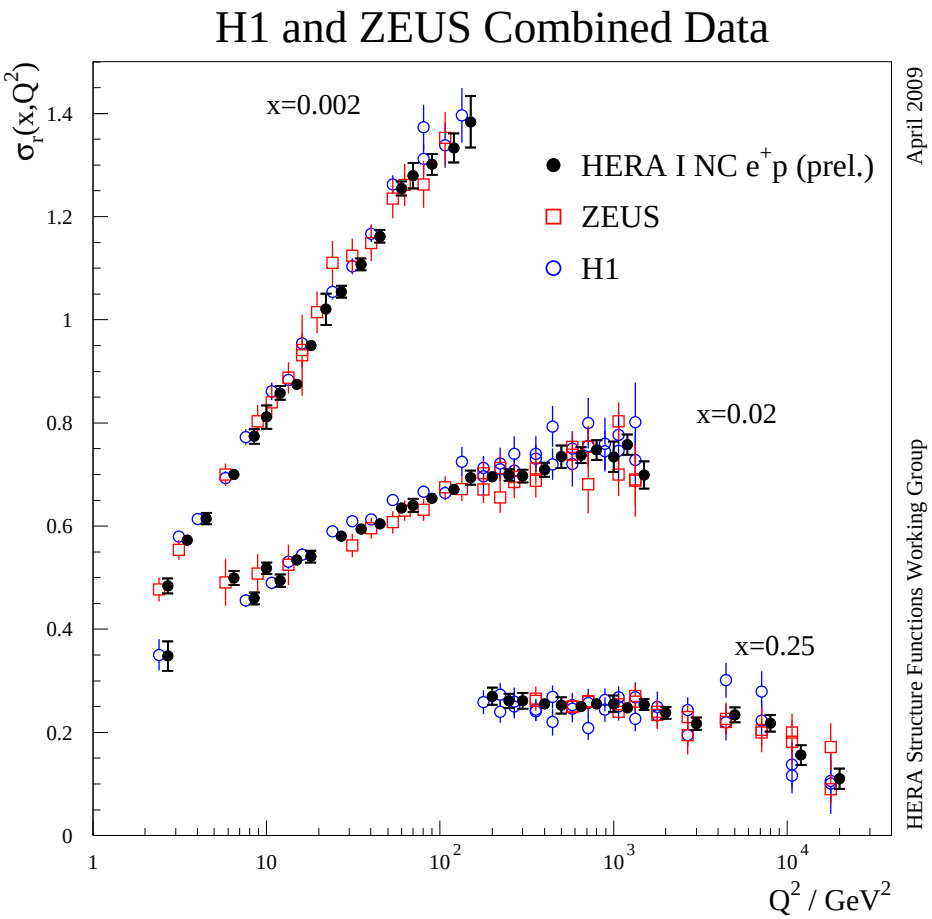

Ultimate precision is obtained by combining H1 and ZEUS measurements.

Average H1 and ZEUS data before applying QCD analysis.

Achieved by fitting σ_r values, global normalisations and the correlated systematic uncertainties.

$$\sigma_r^{\pm} = F_2 - \frac{y^2}{Y_+} \mp \frac{Y_-}{Y_+} xF_3$$

Experiments cross calibrate each other: total uncertainties reduced, sometimes better than $\sqrt{2}$.

$$\chi^2_{\text{exp}}(\boldsymbol{m},\boldsymbol{b}) = \sum_i \frac{\left[m^i - \sum_j \gamma^i_j m^i b_j - \mu^i\right]^2}{\delta^2_{i,\text{stat}}\,\mu^i\left(m^i - \sum_j \gamma^i_j m^i b_j\right) + \left(\delta_{i,\text{uncor}}\, m^i\right)^2} + \sum_j b_j^2.$$

Combined HERA data

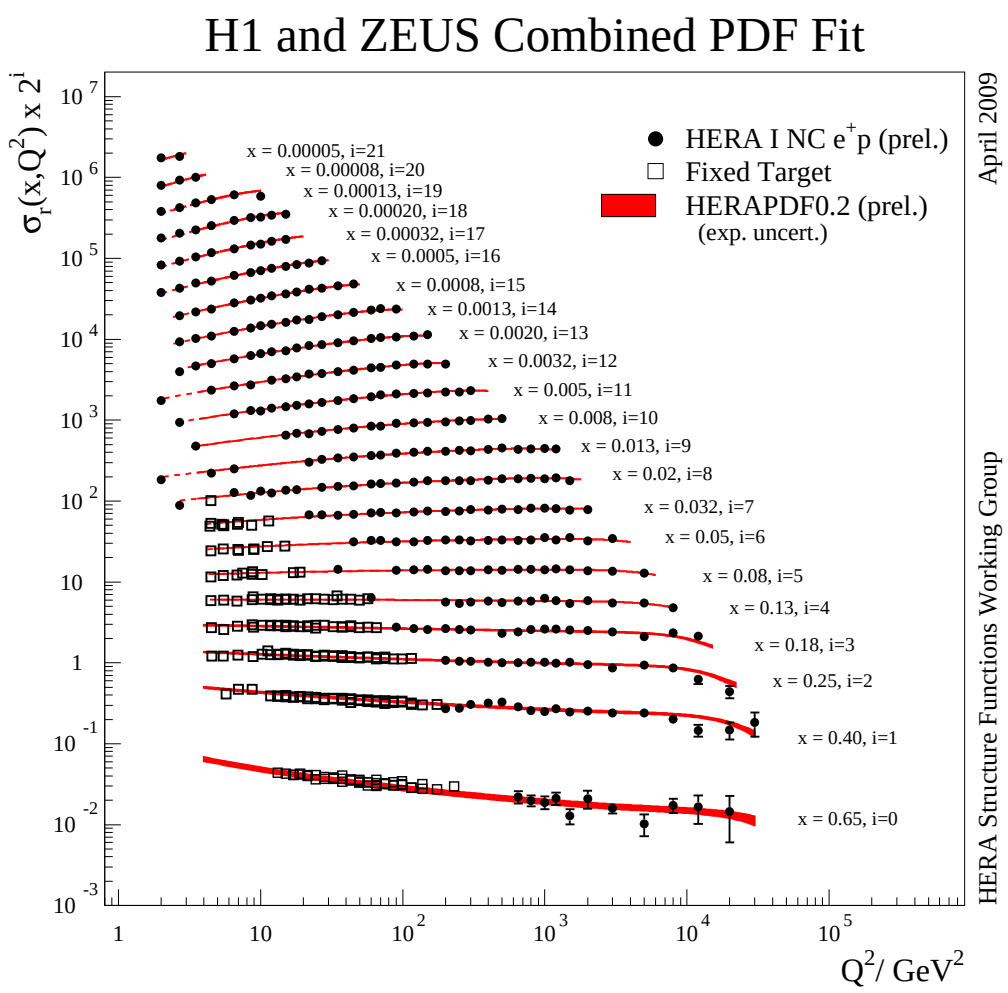

Combination of the published H1/ZEUS data collected at HERA-I for CC,NC, $e^{\pm}p$ mode. 14 publications, 1397 input and 741 output σ_r measurements, 110 correlated experimental error sources. For NC e^+p, $6 \cdot 10^{-7} < x < 0.65$ and $0.045 < Q^2$ 30000 GeV^2.

Combination:

$$\chi^2/dof = 637/656$$

QCD Fit (to the combined HERA data with $Q^2 \geq 3.5$ GeV^2):

$$\chi^2/dof = 574/582$$

HERA data precision is similar to fixed target experiments. Good consistency between H1 and ZEUS. Stringent test of DGLAP evolution.

QCD analysis of the HERA combined data

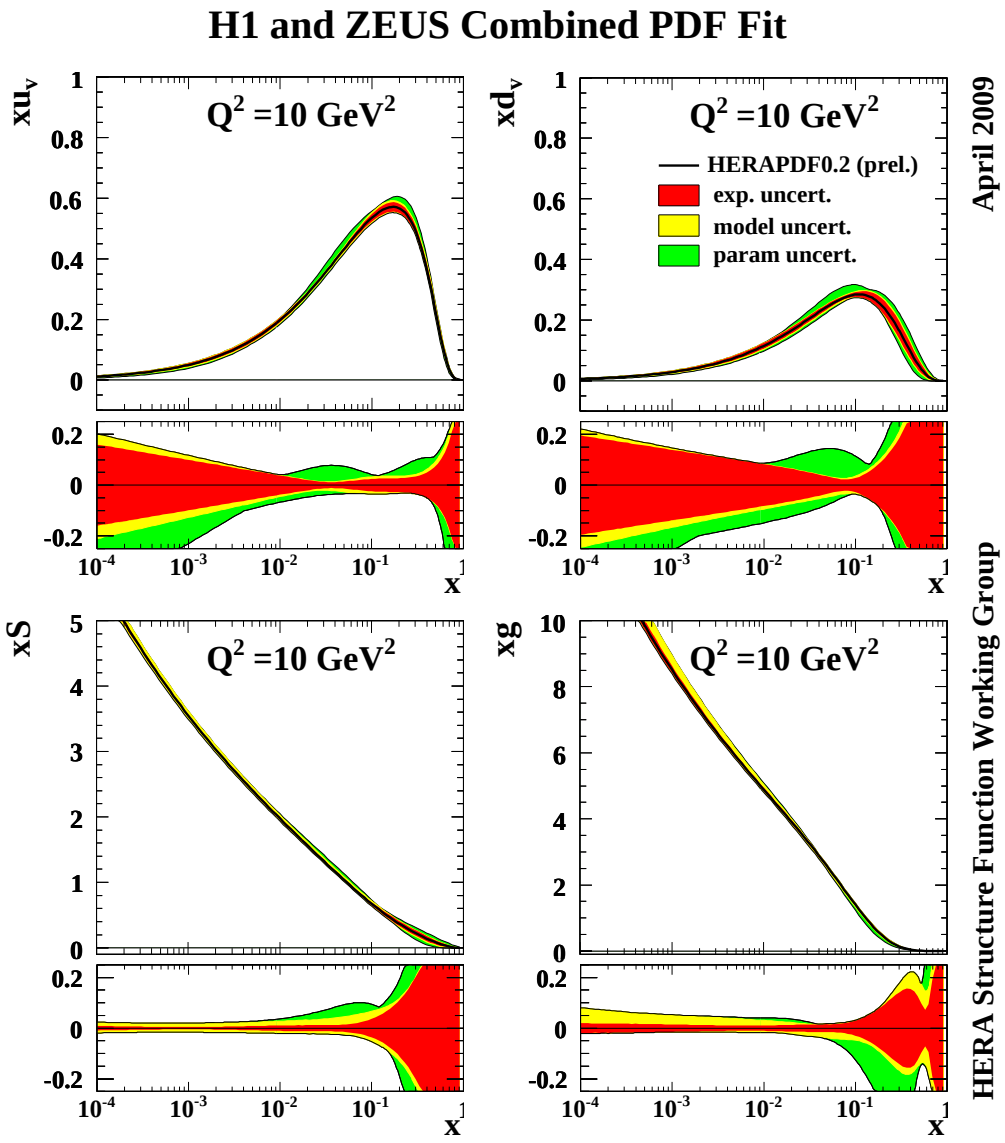

HERAPDF0.2 — NLO QCD analysis of the combined HERA data.

Separation of experimental, model and parameterisation uncertainties, similar to H1PDF2009.

Accurate xS and xg at low x due to precise measurement of F_2.

HERAPDF0.2 compared to Global QCD Fits

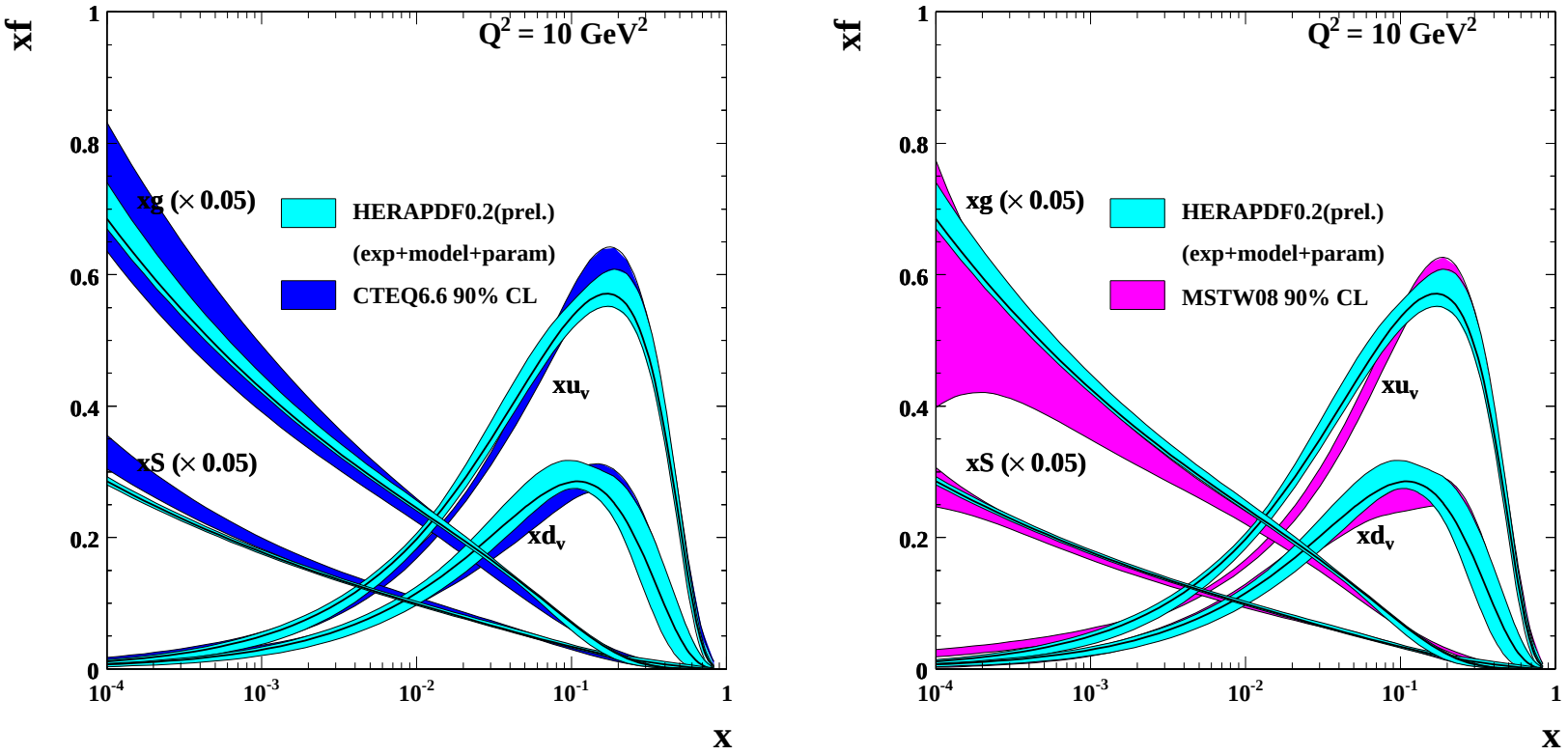

At low x HERAPDF0.2 is more precise for $xS(x)$, $xg(x)$ vs global fits of CTEQ and MRST:

- Global fits don't include the combined HERA/recent H1 data.
- Different error treatment — ongoing discussion in PDF4LHC workshop meetings.

NC Cross Section at high Q^2

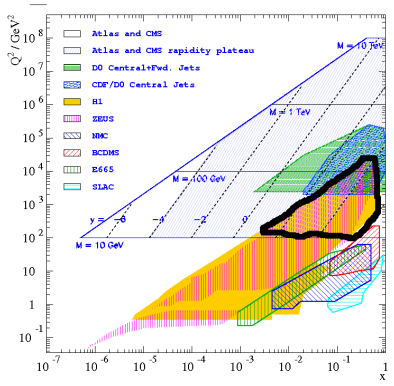

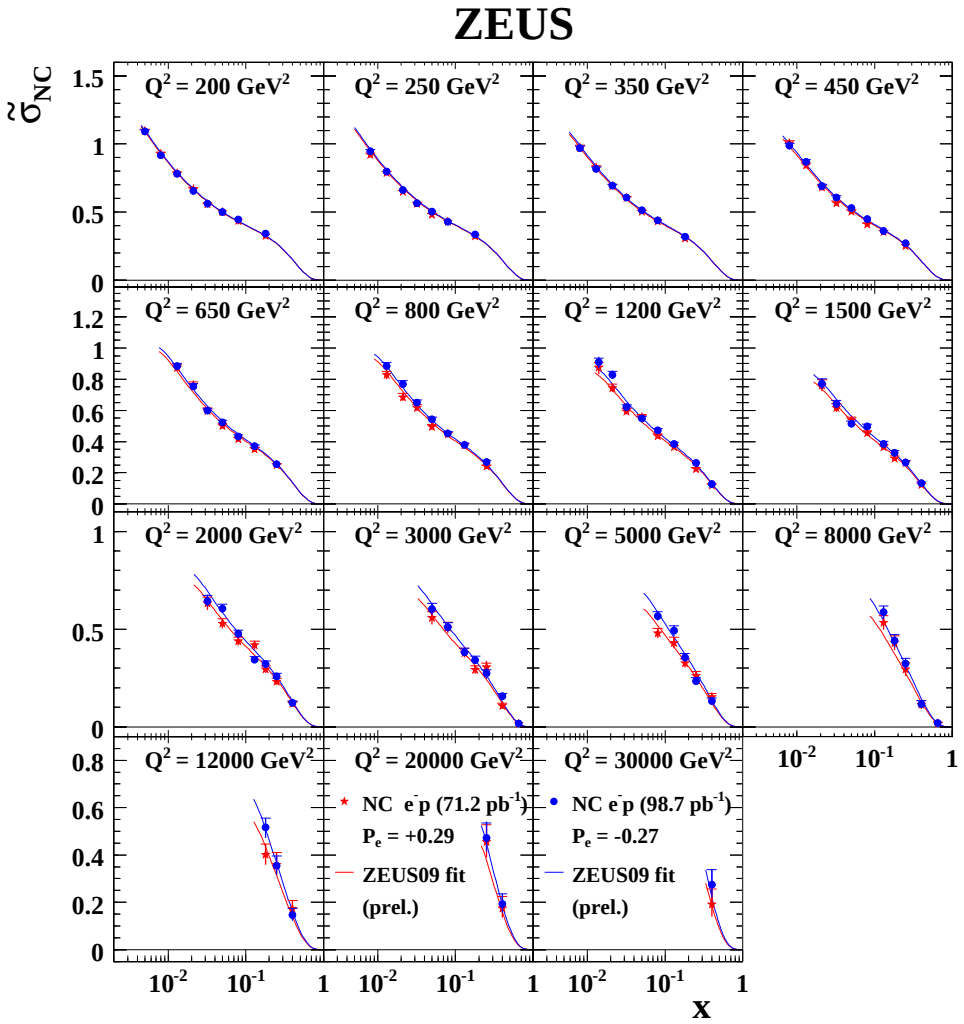

Neglecting pure Z exchange term, generalised F_2:

$$F_2^{\pm} \approx F_2^{\gamma} + k(-v_e \mp Pa_e)F_2^{\gamma Z}$$

where $k = \frac{1}{4\sin^2\theta_W \cos^2\theta_W} \frac{Q^2}{Q^2+M_Z^2}$

At leading order

$$F_2^{\gamma Z} = x\sum 2e_q v_q (q + \bar{q}).$$

Polarisation asymmetry is parity violating.

DESY-08-202, accepted by EPJC.

Complete $e^- p$ HERA-II sample

Charged Current Cross Section

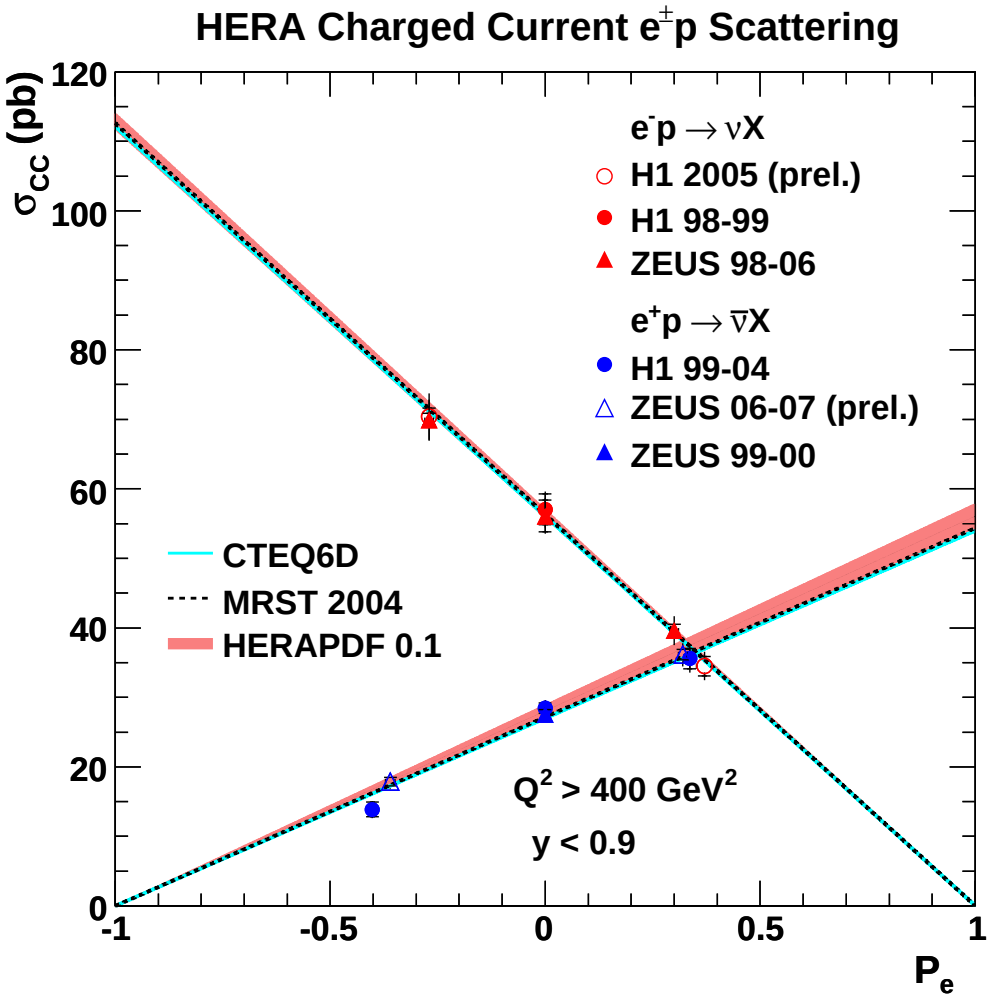

CC cross section is linearly proportional to the degree of the longitudinal $e^{\pm}$ beam polarisation. Consistent with no right-handed weak currents

Double Differential CC Cross Section

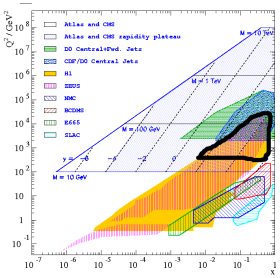

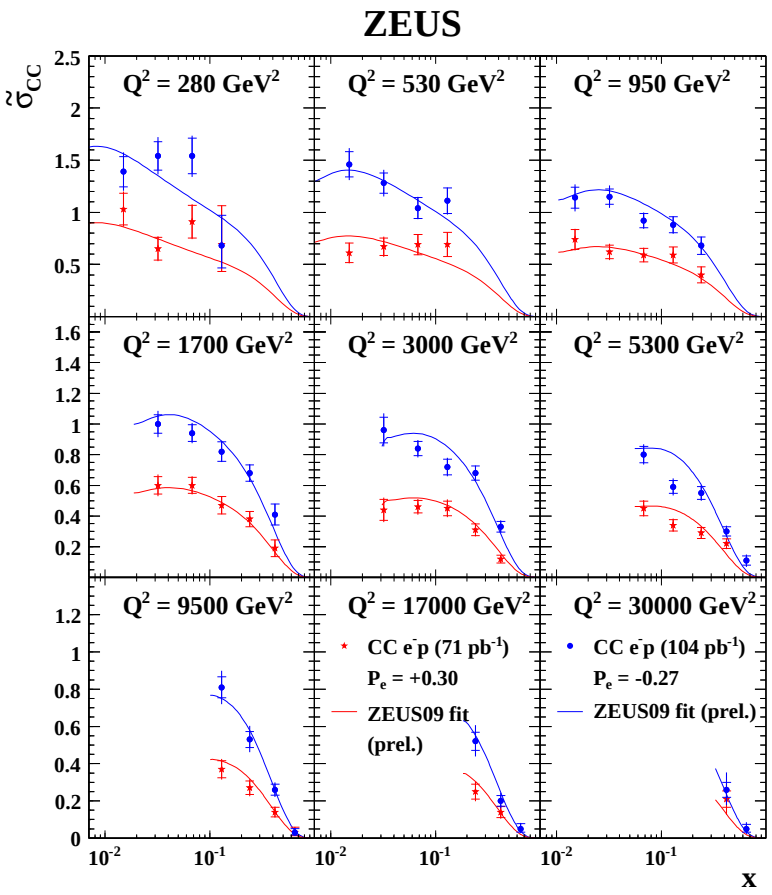

e^-p

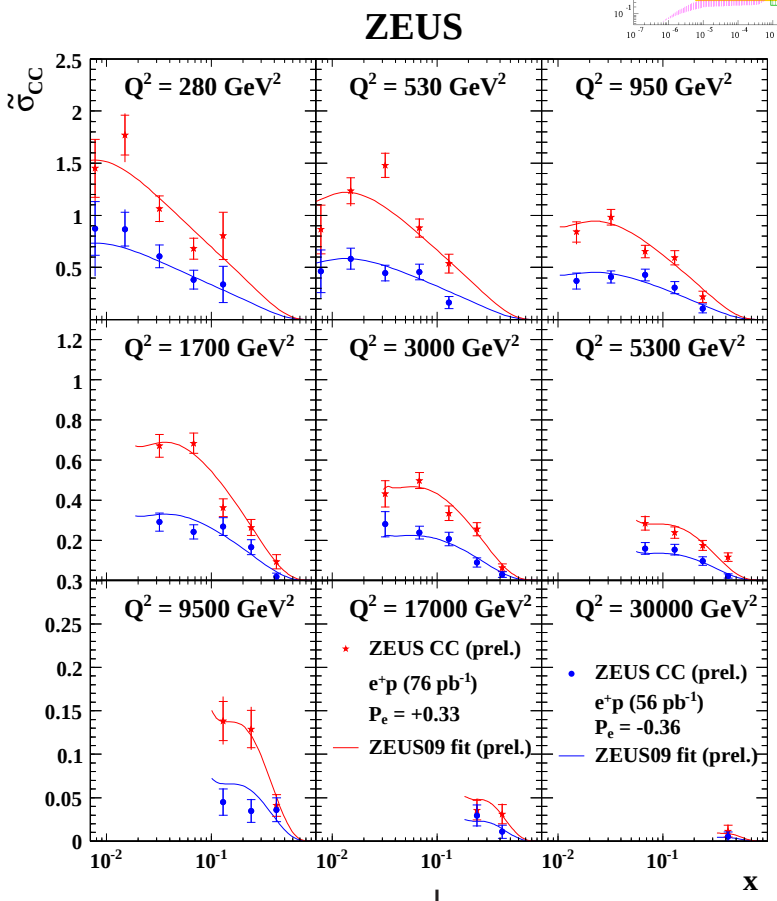

e^+p

CC data allows to measure $D = d + s + b$, $\bar{U} = \bar{u} + \bar{c}$ (for e^+p) and $U = u + c$, $\bar{D} = \bar{d} + \bar{s} + \bar{b}$ (for e^-p).

DESY-08-177, accepted by EPJ C.

Complete HERA-II e^-p sample

Measurement of Strange density, $xs(x)$, by HERMES

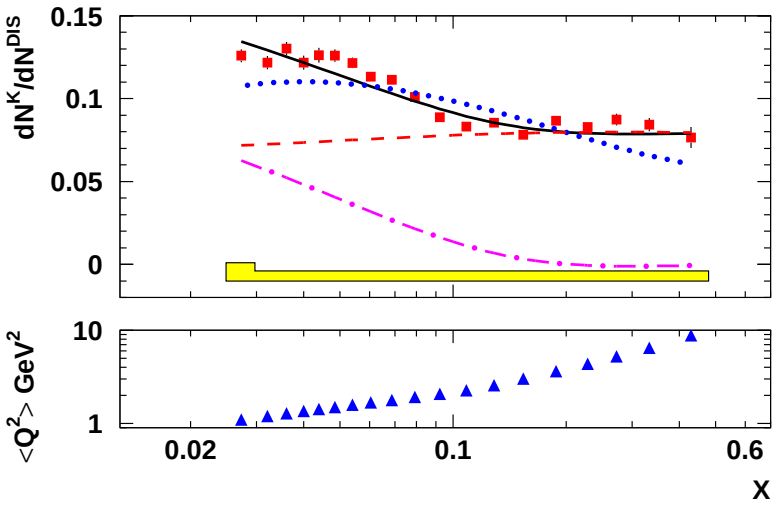

Measure $K^{\pm}$ production on deuteron target compared to inclusive DIS.

$$S(x)\int D_S^K(z)dz \approx Q(x)\left[5\frac{d^2N^K(x)}{d^2N^{DIS}(x)} - \int D_Q^K(z)dz\right]$$

Based on flatness of $dN^K(x)/dN^{DIS}(x)$ for high x, assume $S(x) = 0$ for $x > 0.15$, measure the fragmentation function $\int D_Q^K(x)dz$.

Subtracting the contribution of $\int D_Q^K(x)dz$, evolving to Q^2=2.5 GeV^2 and using an external value of the fragmentation function $\int D_S^K(x)dz$, $xs(x)$ distribution is obtained:

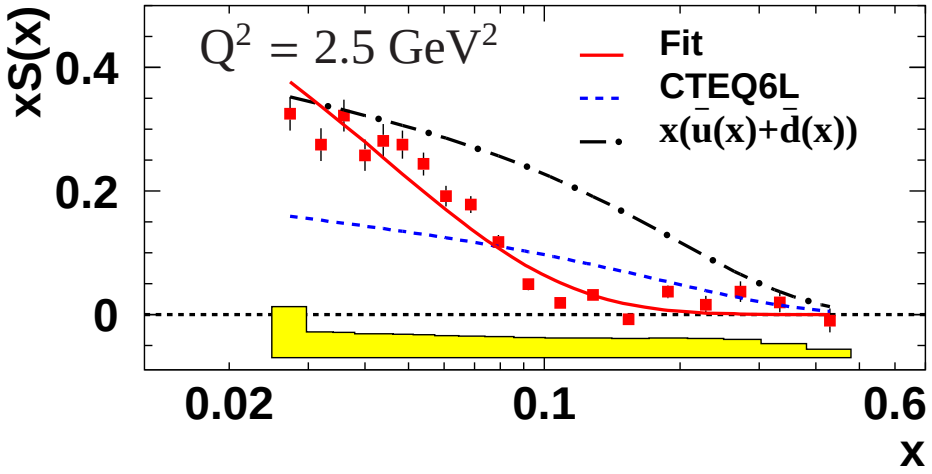

strange PDF seems to have different x dependence vs light quark sea.

Measurements of c, b using displaced vertex.

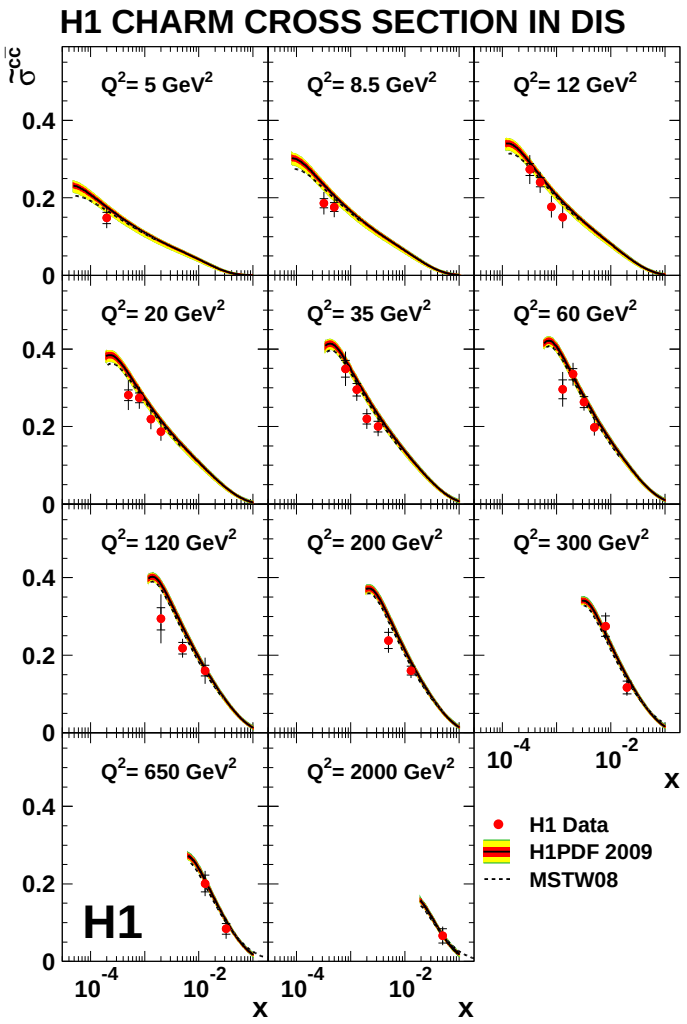

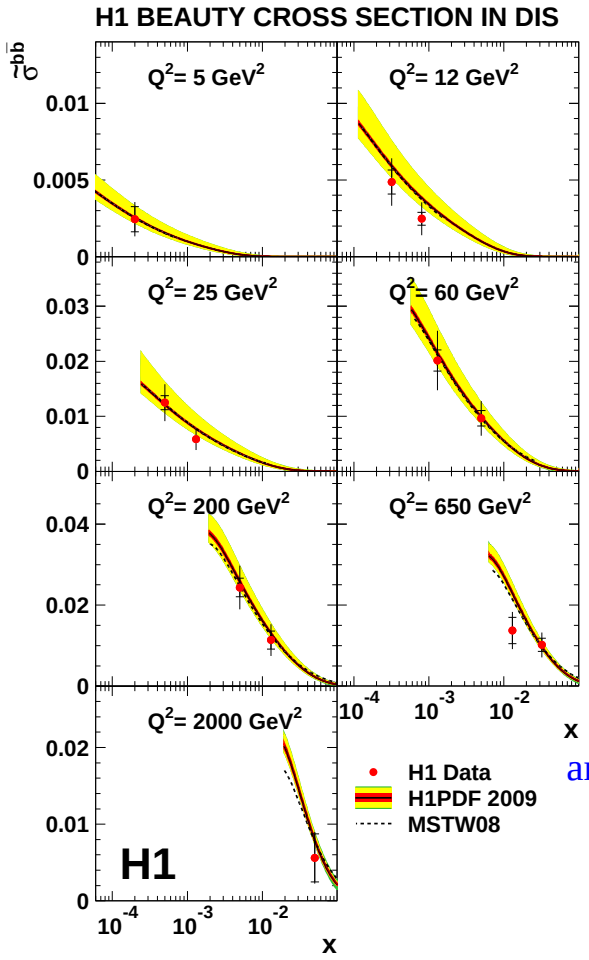

Model uncertainties are dominated by variation of m_c, m_b

arXiv:0907.2643

Complete dataset
$\mathcal{L} = 189\text{pb}^{-1}$

Larger contribution to σ_r ($\equiv \tilde{\sigma}$) allows to determine $\sigma_r^{c\bar{c}}$ more precisely than $\sigma_r^{b\bar{b}}$. Data agree with H1PDF2009 prediction.

Combination of $F_2^{c\bar{c}}$ measurements

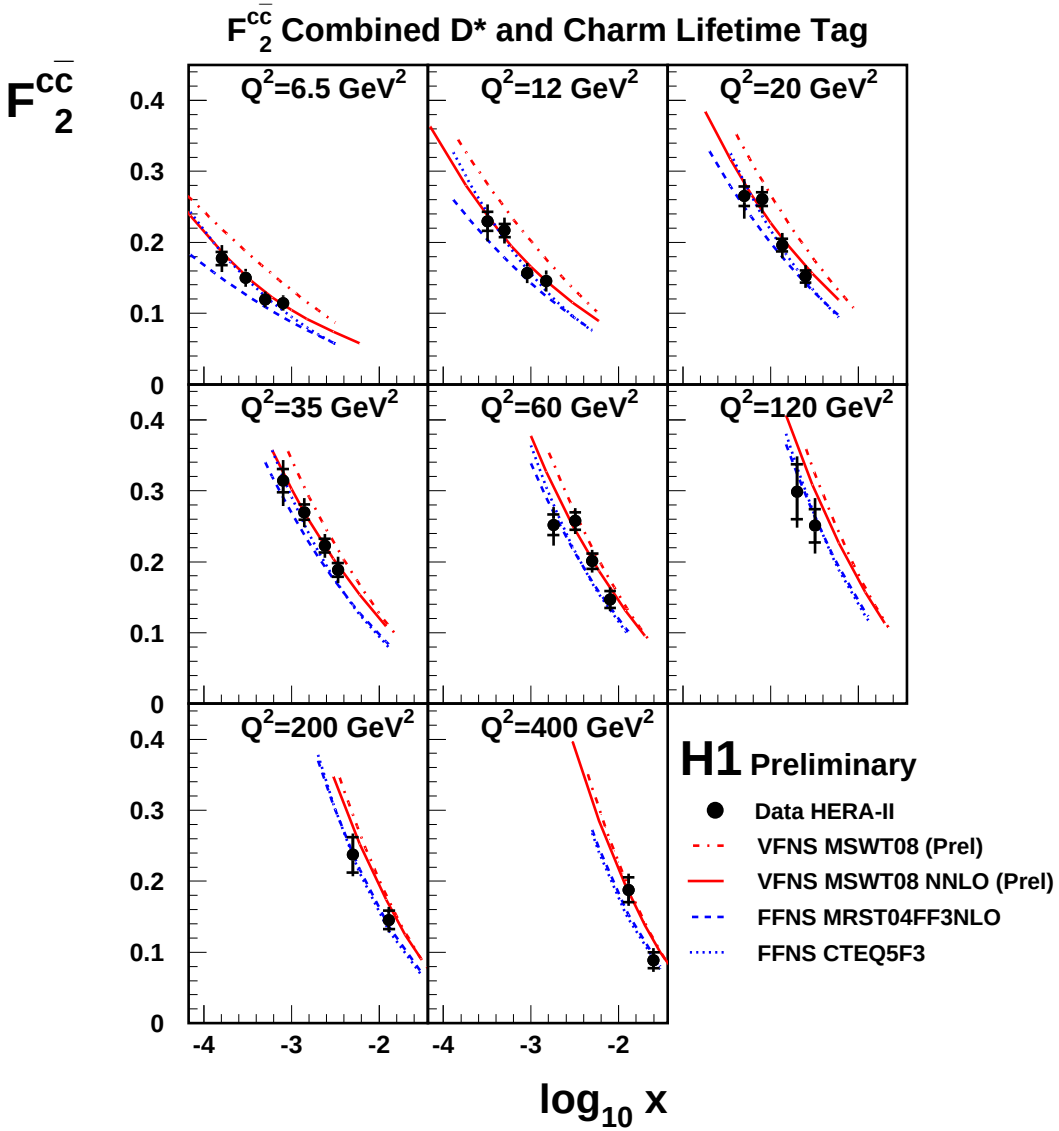

Different methods to measure $F_2^{c\bar{c}}$:

- displaced secondary vertex;
- tagging by measuring D^* meson production.

Methods have different uncertainties: combine taking into account correlations.

→ Significant reduction of the uncertainty.

NLO MSTW08 overshoots the data, NNLO MSTW08 agrees well.

Theory highlights

- Tremendous effort to improve predictions by calculating higher order corrections (LO→NLO→NNLO→N^{3}LO ...).
- Assessment of small *x* effects.
- Improved treatment of heavy flavours.

Very recent NNLO analysis of DIS/Drell-Yan data with general-mass variable-flavour-number heavy quark treatment by S.Alekhin, J.Blümlein, S.Klein and S.Moch (ABKM), DESY 09-102.

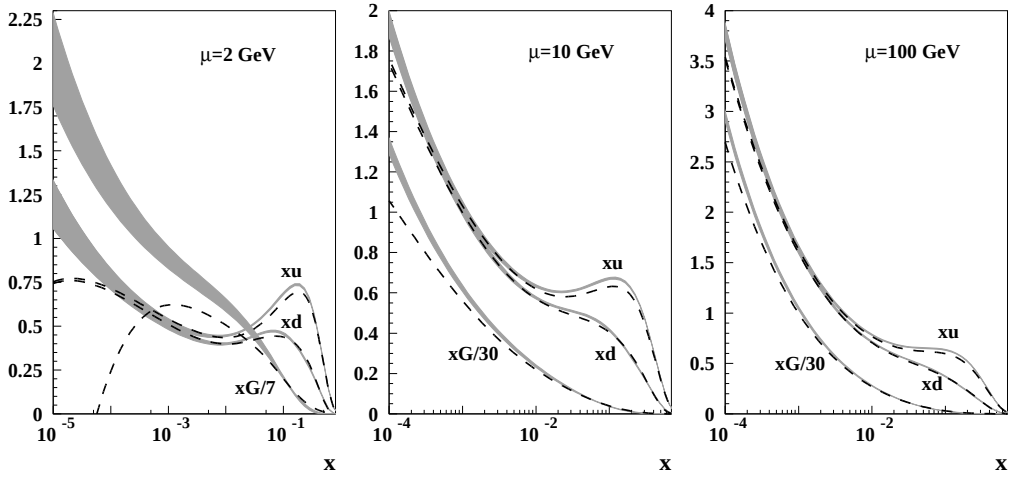

Bands: ABKM analysis, dashed lines: NNLO MSTW08 central values.

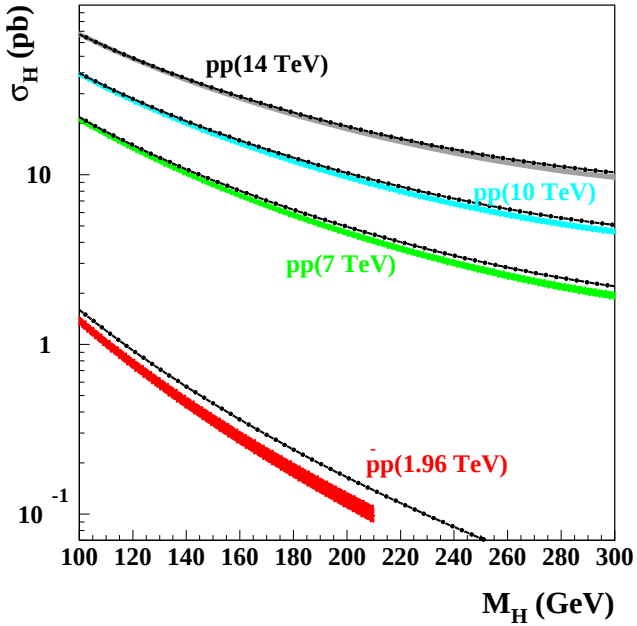

ep Physics Beyond HERA

Successful operation of HERA provided wide variety of fundamental physics results. Still, many questions remain unanswered.

- The spin structure of the proton at low x: p-beam polarisation.
- Light flavour decomposition at low x: ed running.
- Low x structure of heavy nuclei: eA running.
- Saturation of parton densities and relevance of BFKL dynamics: extended x range.
- High statistics elector-weak tests, precise decomposition of parton densities using charged current process: high luminosity and high centre-of-mass energy
- Physics beyond SM in ep interactions: high luminosity and high centre-of-mass energy

These questions are planned to be addressed by proposed high intensity medium (EIC) and high energy (LHeC) ep colliders.

Medium energy *ep* collider EIC: eRHIC and ELIC

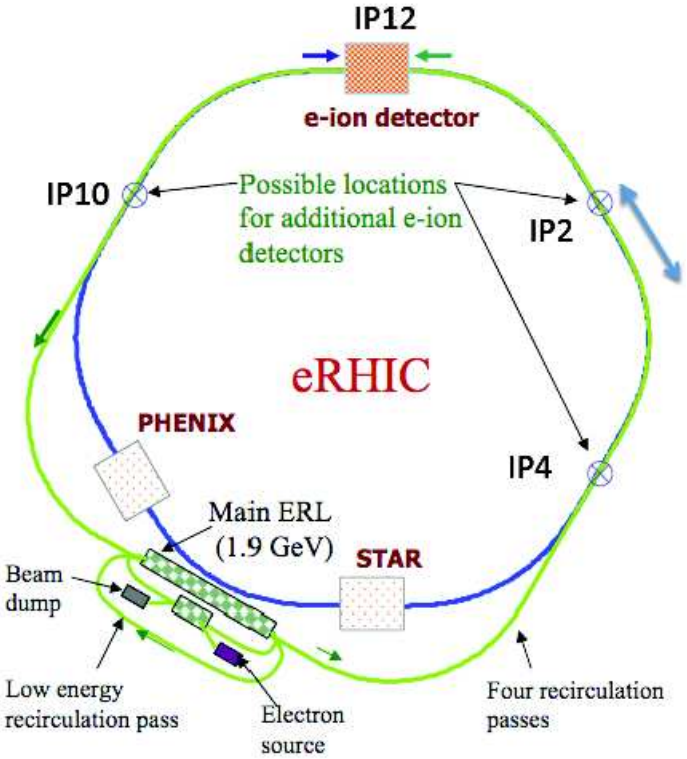

Jlab ELIC, using E_e = 12 GeV. Stages in $E_p \times E_e$ of 5×5, 30×5, 30×10 GeV^2.

Nominal operation at 250×10 GeV^2.

Luminosity: 0.5-4.5 $\times 10^{33}$ cm^{-2}s^{-1}

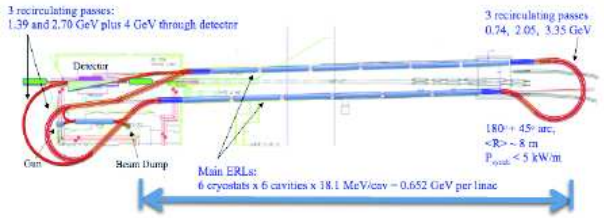

BNL eRHIC staged design, using E_p = 250 GeV:

- E_e = 4 GeV linac
- E_e = 10 – 20 GeV ring, up to E_e = 30 GeV.

Luminosity: 3×10^{33} cm^{-2}s^{-1}.

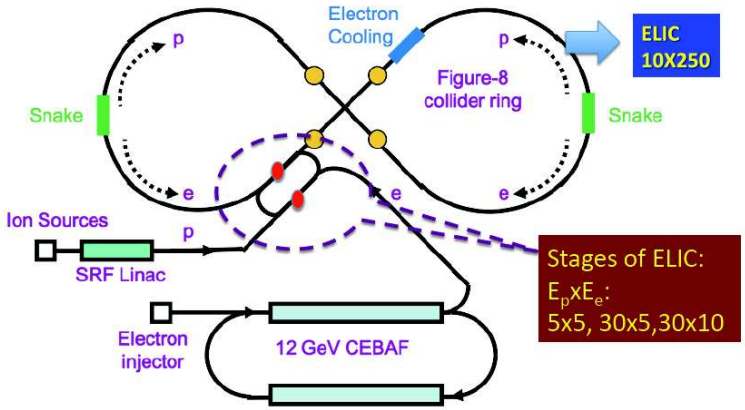

Examples of Physics at EIC

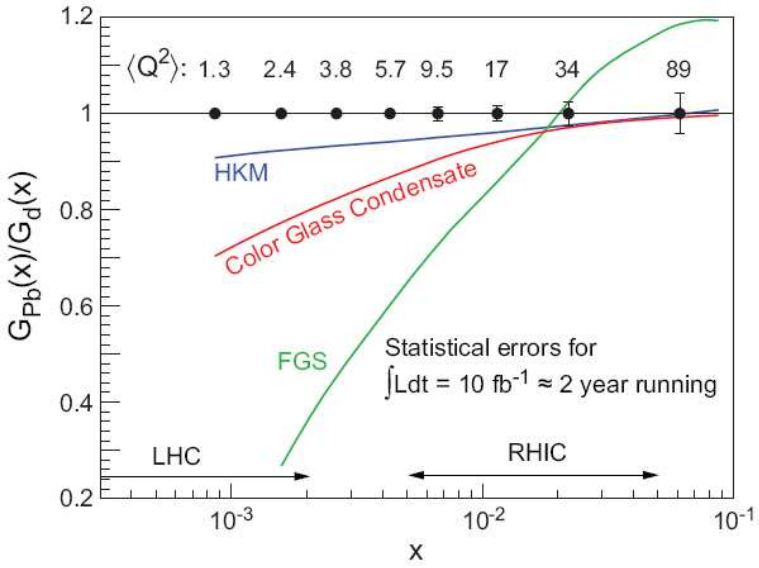

Determine $xg(x, Q^2)$ vs A by measuring $F_L(A, x, Q^2)$. Requires runs at different S. Allows to distinguish among "standard" shadowing (HKM,FGS) and Colour Glass Condensate models.

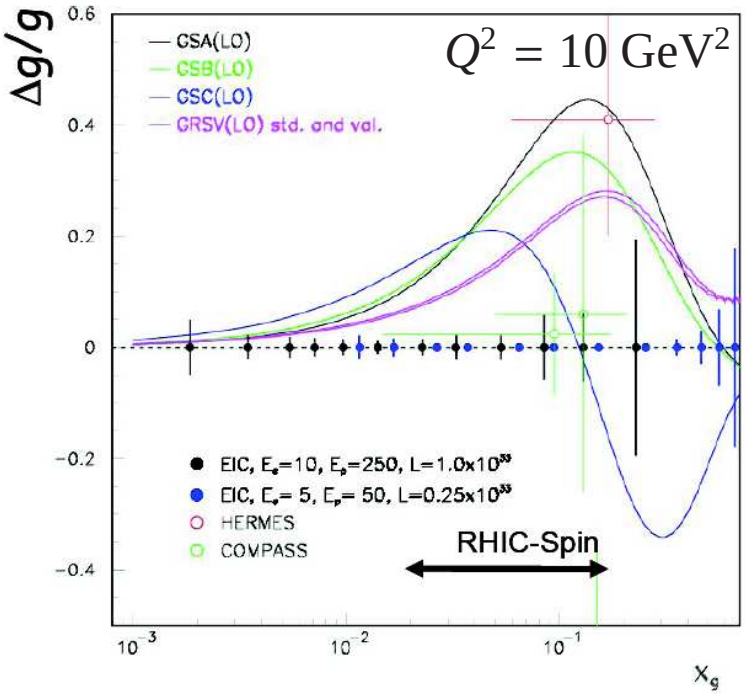

Measure Δg via g_1 scaling violation, exclusive final states.
Example of $\Delta g/g$ determined using tagged charm production which allows to measure with uncertainties smaller than 0.01.

High energy *ep* collider LHeC

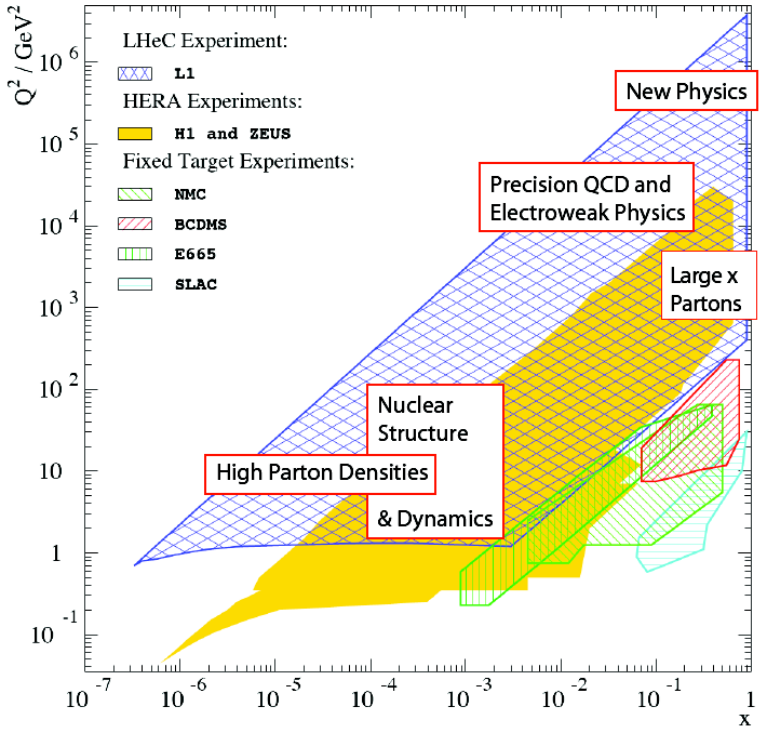

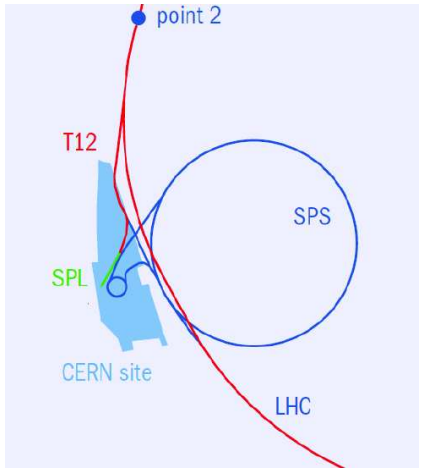

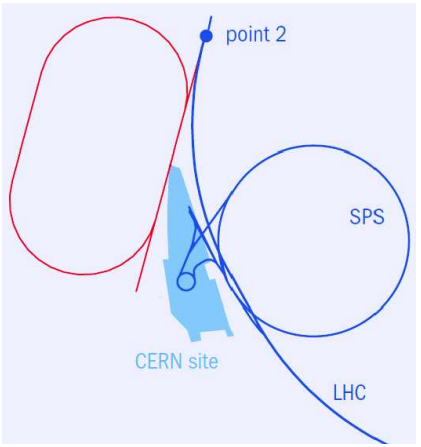

Nominal $E_e \times E_p = 70 \times 7000\,\mathrm{GeV}^2$.
Two designs, ring-ring and ring-linac.

Luminosity: $5 \times 10^{33}\ \mathrm{cm}^{-2}\mathrm{s}^{-1}$

New dedicated detector for high precision physics based on HERA, LHC, ILC experience and designs.
Flexible collider, *p*/*A* and $e^{\pm}$ beams, longitudinal lepton beam polarisation are ideal for QCD/EW studies, BSM searches.

Complementary *ep* machine at the Terascale

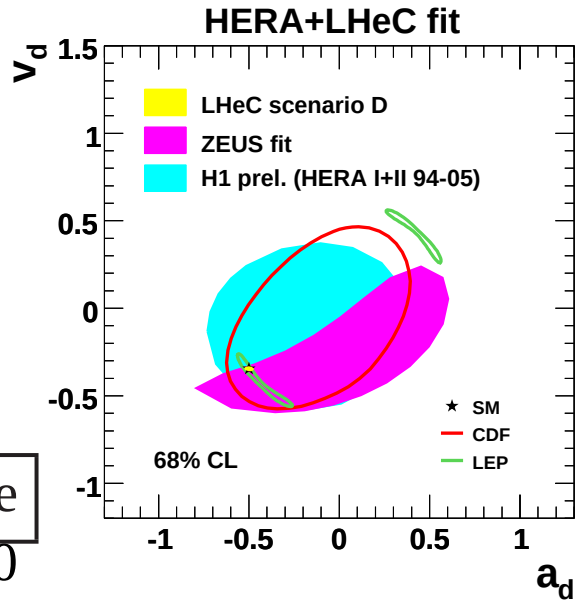

Summary

- Combination of H1 and ZEUS published HERA-I data gives ultimate precision at low x.
- First measurements of F_L at low x.
- Results based on complete HERA sample improve precision at high Q^2.
- New determination of α_S based on jet cross section measurement.
- New results for s, c, b PDFs.
- Precision NLO QCD analyses and novel fit techniques: more reliable predictions for the LHC.
- New colliders at Jlab, BNL and CERN are being developed for polarised and high Q^2/low x ep physics.

  $\rightarrow$ DIS has great future as part of HEP exploring the Terascale.